UNSYS digital

Journal of Unmanned System Technology

Multi-body Dynamics Modeling of Fixed-Pitch Coaxial Rotor Helicopter

Satoshi Suzuki[†], Takahiro Ishii[‡], Gennai Yanagisawa[§], Kazuki Tomita[£], Yasutoshi Yokoyama[§]

[†]Young Researchers Empowerment Center, Shinshu University
Tokida, Ueda-shi, Nagano, Japan

[‡]Graduate School of Science and Technology, Shinshu University
Tokida, Ueda-shi, Nagano, Japan

[§]Gen Corporation
Sasaga, Matsumoto-shi, Nagano, Japan

[£]Engineering System
Sasaga, Matsumoto-shi, Nagano, Japan

***Abstract*—** In this study, a mathematical model of a fixed-pitch co-axial rotor unmanned helicopter is derived by using a multi-body dynamics modeling technique. First, we consider the helicopter as a rigid body system which consists of 2 rigid bodies. The velocity transformation method, which is one of the multi body dynamics technique, is applied to derive equation of motion of the helicopter. All the forces and moments impressed into the helicopter are derived in consideration of the aerodynamics of co-axial rotors. Derived mathematical model of the helicopter is verified by comparing the flight experiment data with model output. Finally, fundamental motion analysis using the model is conducted to establish the motion characteristics of the helicopter.

***Keywords*—** co-axial rotor helicopter, multi-body dynamics modeling, motion analysis.

I. Introduction

In recent years, unmanned helicopter has become to be developed and used for various practical purposes such as aerial photography, surveillance, and crop dusting. Unmanned helicopters are safer and more convenient than manned helicopters, and they can be potentially employed in a wide range of applications. There are many types of unmanned helicopters, which have various sizes, weights, and have various mechanisms. For example, single-rotor type helicopter [1], tilt-rotor type [2], co-axial rotor type [3], and multi-rotor (quad or more) type [4]. In this study, we propose a fixed-pitch co-axial rotor unmanned helicopter, which has specific mechanisms. The fixed-pitch co-axial rotor helicopter has some advantages compared with any variable-pitch rotor type or single-rotor type helicopters. For example, the simplicity of the mechanisms, well maintainability, and well energy conversion efficiency are part of the advantages of our helicopter. Because of these advantages, fixed-pitch co-axial rotor mechanism has been adopted for world smallest manned helicopter shown in **Figure 1**.

Corresponding author: Satoshi Suzuki (e-mail: s-s-2208@shinshu-u.ac.jp)

This paper was originally presented at The 7th International Conference on Intelligent Unmanned Systems, Chiba, Japan, on Oct 31 – Nov 2, 2011.
It was submitted on February 21, 2013; revised on May 3, 2013; and accepted on May 5, 2013.



Figure 1 – Co-axial rotor manned helicopter

For the practical operation, it is important to know how the helicopter behaves in flight, and it is also important to know how we should coordinate the mechanical parameters to improve the behavior of the helicopter. Moreover, precise mathematical model of the helicopter is necessary to design the autonomous control system for our helicopter. However, modeling and motion analysis of fixed-pitch co-axial rotor helicopter has not been studied so far because the helicopter has some specific mechanisms such as fixed-pitch co-axial rotor, rotor tilting mechanism, and a mechanism for shifting the center of the mass.

In this paper, a mathematical model of fixed-pitch co-axial rotor unmanned helicopter is derived to know how the helicopter behaves in flight. A multi-body dynamics modeling technique named velocity transformation method is adopted to derive an equation of motion. Numerical simulation is performed to compare the output of the derived model with experimental data, and validity of the model is shown. In the simulation, all the forces and moments impressed into the helicopter are derived in consideration of the aerodynamics of co-axial rotors. Finally, fundamental motion analysis is

performed using the model to establish the relation between the motion and the mechanical specification of the helicopter. The main contribution of this paper is that the fixed-pitch co-axial rotor unmanned helicopter with novel mechanical specification is proposed and modeled. The rest of this paper is organized as follows. The overview of our fixed-pitch co-axial rotor unmanned helicopter is introduced in section II. The equation of motion of the helicopter is derived and verified in section III. In section III.A, a fundamental motion analysis is performed using the derived model. Finally, the conclusion of this paper is shown in section V.

II. Fixed-Pitch Co-Axial Rotor Unmanned Helicopter

Figure 2 shows an overview of our co-axial rotor unmanned helicopter. The main specifications of this helicopter are listed in **Table 1**. This helicopter has four 125 cc gasoline engines for a source of power and could lift large payload approximately 100 kg because it was originally designed for manned helicopter. Because of this large payload capacity, the helicopter is expected to be applied to various industrial tasks not only information gathering such as aerial photography but also transportation of heavy goods. Most important features of this helicopter are to have a fixed-pitch co-axial rotor as shown in **Figure 3**. The mechanisms of the rotor segment are simpler than which of any other co-axial rotor helicopters [6] by this feature. This simplicity conducts a reduction of parts count, and improvement of the maintainability. Moreover, the size of this helicopter is small, and the energy conversion efficiency is better than single-rotor type helicopters because it does not have tail rotor. Meanwhile, the fixed-pitch helicopter has a disadvantage in forward flight, called pitch-up phenomenon. In forward flight, relative wind blows into the rotor disc, and causes imbalance of lift force on the disc. Then, this imbalance generates aerodynamic moment, which lifts the nose of the helicopter. In the case of variable-pitch helicopter, the imbalance can be canceled out by cyclic pitch control. By contrast, fixed-pitch helicopter cannot cancel out this imbalance, and the nose of the helicopter is lifted, and then the forward velocity decreases. Therefore, the maximum cruise speed of the fixed-pitch helicopter may be smaller than the speed of the variable-pitch helicopter. It is a serious problem for practical tasks. To solve the above mentioned problem, we have proposed the mechanism for shifting the center of mass of the helicopter.

The entire mechanism of our helicopter is shown in **Figure 4**. The helicopter is divided into two parts, the mission unit and the frame unit, and two units are connected by the universal joint. The mission unit consists of co-axial rotor and gasoline engine, the frame unit consists of fuel tanks and the electric devices for control. There are two mechanisms near the universal joint. The tilting mechanism directly tilts the rotor disc by using four servo motors to generate the horizontal force. The shifting mechanism changes horizontal position of the frame unit relative to the mission unit, and so the center of the mass of the helicopter shifts, and the moment of a couple is generated by gravitational force and the rotor thrust. This moment is used for canceling out the pitch-up moment in forward flight.



Figure 2 – Co-axial rotor unmanned helicopter



Figure 3 – Fixed-pitch co-axial rotors

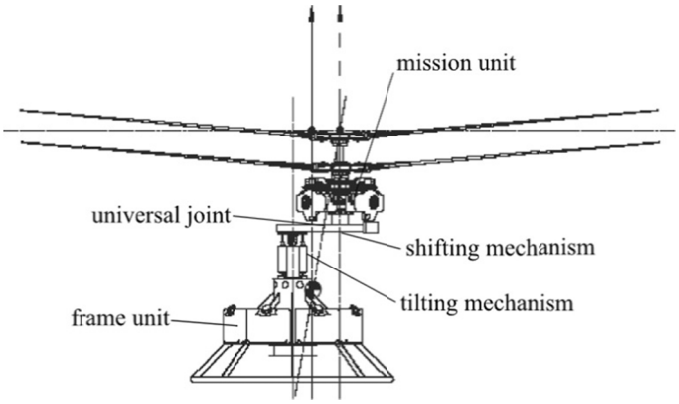


Figure 4 – Mechanisms of the helicopter

Table 1 – Specifications of Unmanned Helicopter

Rotor diameter	4000 [mm]
Height	1600 [mm]
Weight	166 [kg]
Source of power	Gasoline Engine
Endurance	1 [h]
Payload	Approximately 100 [kg]

III. MODELING

In this section, we derive the mathematical model of our fixed-pitch co-axial rotor unmanned helicopter. To derive the mathematical model of the helicopter, we consider the helicopter as a rigid model which consists of 2 rigid bodies. We apply the velocity transformation method to derive nonlinear equations of motion of the helicopter. We assume that all the forces and moments impressed into the helicopter are generated by co-axial rotors, and we derive them in consideration of rotor aerodynamics. First, the velocity transformation method is briefly introduced, and we apply this method to our helicopter, and the nonlinear equation of motion is derived.

A. Velocity Transformation Method

The velocity transformation method is one of the multi-body dynamics technique proposed by Tajima ([7]), and it is similar to a traditional velocity transformation technique. In the following, the outline of the velocity transformation method is described. The detail of the method is presented in [7], and the details of the velocity transformation technique also appear in [8]-[10]. First, the generalized velocity of a rigid body without constraint is considered as $\boldsymbol{H}$. Then the equation of motion of the rigid body is represented as

$$\boldsymbol{m}^H \dot{\boldsymbol{H}} = \boldsymbol{f}^H \tag{1}$$

Here, $\boldsymbol{m}^H$ is a symmetric matrix representing the inertia of the rigid body, $\boldsymbol{f}^H$ is the external force, which is impressed on the rigid body. If some mechanical constraints are added to the rigid body, **(1)** is rewritten as

$$\boldsymbol{m}^H \dot{\boldsymbol{H}} = \boldsymbol{f}^H + \bar{\boldsymbol{f}}^H \tag{2}$$

Here, $\bar{\boldsymbol{f}}^H$ represents the constraint force. On the other hand, a generalized velocity of a rigid body with constraint is considered as $\boldsymbol{S}$, and the equation of the motion is obtained as

$$\boldsymbol{m}^S \dot{\boldsymbol{S}} = \boldsymbol{f}^S \tag{3}$$

Here, $\boldsymbol{m}^S$ represents the inertia matrix, and $\boldsymbol{f}^S$ represents the external force vector. Now, in the case of holonomic and simple non-holonomic system, the relation between generalized velocities $\boldsymbol{H}$ and $\boldsymbol{S}$ is obtained as follows:

$$\boldsymbol{H} = \boldsymbol{H}_S \boldsymbol{S} + \boldsymbol{H}_{\bar{S}} \tag{4}$$

Here, $\boldsymbol{H}_S$ and $\boldsymbol{H}_{\bar{S}}$ are appropriate matrices. Calculating the time derivatives of **(4)**, and substituting it into **(2)**, following equation could be obtained.

$$\boldsymbol{H}_S^{\mathrm{T}} \boldsymbol{m}^H \boldsymbol{H}_S \dot{\boldsymbol{S}} = \boldsymbol{H}_S^{\mathrm{T}} \left\{ \boldsymbol{f}^H - \boldsymbol{m}^H \left(\frac{d\boldsymbol{H}_S}{dt} \boldsymbol{S} + \frac{d\boldsymbol{H}_{\bar{S}}}{dt} \right) + \bar{\boldsymbol{f}}^H \right\} \tag{5}$$

According to [7], it can be easily shown that $\mathbf{H}_S^{\mathrm{T}} \bar{\mathbf{f}}^H$ is equal to zero. Therefore, comparing **(3)** and **(5)**, $\boldsymbol{m}^S$ and $\boldsymbol{f}^S$ is expressed by using $\boldsymbol{m}^H$ and $\boldsymbol{f}^H$ as follows:

$$\boldsymbol{m}^S = \boldsymbol{H}_S^{\mathrm{T}} \boldsymbol{m}^H \boldsymbol{H}_S \tag{6}$$

$$\boldsymbol{f}^S = \boldsymbol{H}_S^T \left\{ \boldsymbol{f}^H - \boldsymbol{m}^H \left(\frac{d\boldsymbol{H}_S}{dt} \boldsymbol{S} + \frac{d\boldsymbol{H}_{\bar{S}}}{dt} \right) \right\} \tag{7}$$

If $\boldsymbol{m}^H$ and $\boldsymbol{f}^H$ were given and the relation **(4)** could be derived, the equation of motion of rigid bodies with constraints could be obtained by using **(3)**, **(6)**, and **(7)**. This method includes the velocity transformation **(4)**, therefore the method is called velocity transformation method.

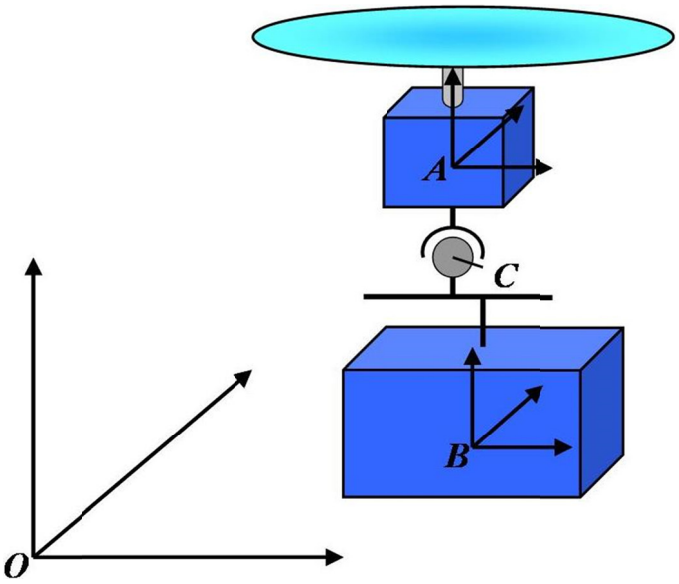


Figure 5 – Coordinate systems

B. Equation of Motion of Co-Axial Rotor Helicopter

The equation of motion of the co-axial rotor helicopter is derived. Coordinate systems used in this section are defined in **Figure 5**. The ***O***-frame is an inertial frame fixed at an arbitrary point on the ground, ***A***-frame is fixed on the mission unit, and ***B***-frame is fixed on the frame unit. ***A***-frame and ***B***-frame are movable coordinate system which moves in conjunction with the motion of each unit. Moreover, the notation ***C*** denotes the universal joint. In these coordinate systems, $\boldsymbol{R}_{OA}$ represents the position of the mission unit relative to the ***O***-frame, and it is expressed as the vector on ***O***-frame. On the other hand, $\boldsymbol{R}'_{OA}$ represents the same vector which is expressed on ***A***-frame. This manner is also applied to linear velocity, angular velocity, and force vector. Moreover, in the case of the frame unit, relative position vector is represented as $\boldsymbol{R}_{OB}$ and $\boldsymbol{R}'_{OB}$. If there was no constraint by the universal joint, the mission unit and the frame unit are regarded as free rigid bodies. Thus, the equation of motion of each unit is represented as follows:

$$\boldsymbol{M}_{\mathrm{A}} \dot{\boldsymbol{V}}'_{\mathrm{OA}} = \boldsymbol{F}'_{\mathrm{OA}} - \boldsymbol{M}_{\mathrm{A}} \tilde{\boldsymbol{\Omega}}'_{\mathrm{OA}} \boldsymbol{V}'_{\mathrm{OA}} \tag{8}$$

$$\boldsymbol{J}_{\mathrm{A}} \dot{\boldsymbol{\Omega}}'_{\mathrm{OA}} = \boldsymbol{N}'_{\mathrm{OA}} - \tilde{\boldsymbol{\Omega}}'_{\mathrm{OA}} \boldsymbol{J}_{\mathrm{A}} \boldsymbol{\Omega}'_{\mathrm{OA}} \tag{9}$$

$$\boldsymbol{M}_{\mathrm{B}} \dot{\boldsymbol{V}}'_{\mathrm{OB}} = \boldsymbol{F}'_{\mathrm{OB}} - \boldsymbol{M}_{\mathrm{B}} \tilde{\boldsymbol{\Omega}}'_{\mathrm{OB}} \boldsymbol{V}'_{\mathrm{OB}} \tag{10}$$

$$\boldsymbol{J}_{\mathrm{B}} \dot{\boldsymbol{\Omega}}'_{\mathrm{OB}} = \boldsymbol{N}'_{\mathrm{OB}} - \tilde{\boldsymbol{\Omega}}'_{\mathrm{OB}} \boldsymbol{J}_{\mathrm{B}} \boldsymbol{\Omega}'_{\mathrm{OB}} \tag{11}$$

Here, $\boldsymbol{M}$ denotes the mass of each unit, $\boldsymbol{J}$, the inertia matrix, $\boldsymbol{V}'$ and $\boldsymbol{\Omega}'$, the linear and angular velocity, and $\boldsymbol{F}'$, $\boldsymbol{N}'$ denote the external force and torque vector. Additionally, $\tilde{\boldsymbol{\Omega}}'$ denotes the skew symmetric matrix which represents vector product. Now, we choose the generalized velocity without constraint as

$$\boldsymbol{H} = \begin{bmatrix} \boldsymbol{V}_{\mathrm{OA}}'^{\mathrm{T}} & \boldsymbol{\Omega}_{\mathrm{OA}}'^{\mathrm{T}} & \boldsymbol{V}_{\mathrm{OB}}'^{\mathrm{T}} & \boldsymbol{\Omega}_{\mathrm{OB}}'^{\mathrm{T}} \end{bmatrix}^{\mathrm{T}} \tag{12}$$

Then, $\boldsymbol{m}^H$ and $\boldsymbol{f}^H$ in **(1)** are obtained from **(8)**-**(11)** as

$$\boldsymbol{m}^H = \begin{bmatrix} \boldsymbol{M}_{\mathrm{A}} & \boldsymbol{O} & \boldsymbol{O} & \boldsymbol{O} \\ \boldsymbol{O} & \boldsymbol{J}_{\mathrm{A}} & \boldsymbol{O} & \boldsymbol{O} \\ \boldsymbol{O} & \boldsymbol{O} & \boldsymbol{M}_{\mathrm{B}} & \boldsymbol{O} \\ \boldsymbol{O} & \boldsymbol{O} & \boldsymbol{O} & \boldsymbol{J}_{\mathrm{B}} \end{bmatrix} \tag{13}$$

$$\boldsymbol{f}^H = \begin{bmatrix} \boldsymbol{F}_{\mathrm{OA}}' - \boldsymbol{M}_{\mathrm{A}}\tilde{\boldsymbol{\Omega}}_{\mathrm{OA}}'\boldsymbol{V}_{\mathrm{OA}}' \\ \boldsymbol{N}_{\mathrm{OA}}' - \tilde{\boldsymbol{\Omega}}_{\mathrm{OA}}'\boldsymbol{J}_{\mathrm{A}}\boldsymbol{\Omega}_{\mathrm{OA}}' \\ \boldsymbol{F}_{\mathrm{OB}}' - \boldsymbol{M}_{\mathrm{B}}\tilde{\boldsymbol{\Omega}}_{\mathrm{OB}}'\boldsymbol{V}_{\mathrm{OB}}' \\ \boldsymbol{N}_{\mathrm{OB}}' - \tilde{\boldsymbol{\Omega}}_{\mathrm{OB}}'\boldsymbol{J}_{\mathrm{B}}\boldsymbol{\Omega}_{\mathrm{OB}}' \end{bmatrix} \tag{14}$$

We consider the constraint of angular velocity as

$$\boldsymbol{\Omega}_{\mathrm{OA}}' = \boldsymbol{C}_{\mathrm{AB}}\boldsymbol{\Omega}_{\mathrm{OB}}' + \boldsymbol{\Omega}_{\mathrm{BA}}' \tag{15}$$

Here, $\boldsymbol{C}_{AB}$ is the coordinate transformation matrix which transforms a vector from $\boldsymbol{B}$-frame to $\boldsymbol{A}$-frame, $\boldsymbol{\Omega}_{AB}'$ is the relative angular velocity of the mission unit to the frame unit, and it is determined by the motion of the tilting mechanism. The constraint of the position is obtained as

$$\boldsymbol{R}_{\mathrm{OA}} = \boldsymbol{R}_{\mathrm{OB}} + \boldsymbol{C}_{\mathrm{OB}}\boldsymbol{R}_{\mathrm{BC}} - \boldsymbol{C}_{\mathrm{OA}}\boldsymbol{R}_{\mathrm{AC}} \tag{16}$$

Here, $\boldsymbol{C}_{OB}$ and $\boldsymbol{C}_{OA}$ are the coordinate transformation matrices. $\boldsymbol{R}_{BC}$ And $\boldsymbol{R}_{AC}$ represent the position of the universal joint, and defined as

$$\begin{aligned} \boldsymbol{R}_{\mathrm{BC}} &= \begin{bmatrix} x_{shift} & y_{shift} & d \end{bmatrix}^{\mathrm{T}} \\ \boldsymbol{R}_{\mathrm{AC}} &= \begin{bmatrix} 0 & 0 & l \end{bmatrix}^{\mathrm{T}} \end{aligned} \tag{17}$$

d is a distance between center of gravity of the frame unit and universal joint, l is the distance between the mission unit and the joint (**Figure 5**). x_{shift} and y_{shift} are determined by the motion of the shifting mechanism. Time derivatives of **(16)** is obtained as

$$\boldsymbol{V}_{\mathrm{OA}} = \boldsymbol{V}_{\mathrm{OB}} - \boldsymbol{C}_{\mathrm{OB}}\tilde{\boldsymbol{R}}_{\mathrm{BC}}\boldsymbol{\Omega}_{\mathrm{OB}}' + \boldsymbol{C}_{\mathrm{OB}}\boldsymbol{V}_{\mathrm{BC}} + \boldsymbol{C}_{\mathrm{OA}}\tilde{\boldsymbol{R}}_{\mathrm{AC}}\boldsymbol{\Omega}_{\mathrm{OA}}' \tag{18}$$

Similarly, $\boldsymbol{V}_{OA}'$ is obtained as

$$\begin{aligned} \boldsymbol{V}_{\mathrm{OA}}' = \boldsymbol{C}_{\mathrm{AB}}\boldsymbol{V}_{\mathrm{OB}}' + (\tilde{\boldsymbol{R}}_{\mathrm{AC}}\boldsymbol{C}_{\mathrm{AB}} - \boldsymbol{C}_{\mathrm{OB}}\tilde{\boldsymbol{R}}_{\mathrm{BC}})\boldsymbol{\Omega}_{\mathrm{OB}}' \\ + \boldsymbol{C}_{\mathrm{AB}}\boldsymbol{V}_{\mathrm{BC}}' + \tilde{\boldsymbol{R}}_{\mathrm{AC}}\boldsymbol{\Omega}_{\mathrm{BA}}' \end{aligned} \tag{19}$$

Here, we used **(15)** to derive **(19)**. Considering the generalized velocity with constraint as

$$\boldsymbol{S} = \begin{bmatrix} \boldsymbol{V}_{\mathrm{OB}}'^{\mathrm{T}} & \boldsymbol{\Omega}_{\mathrm{OB}}'^{\mathrm{T}} \end{bmatrix}^{\mathrm{T}} \tag{20}$$

$\boldsymbol{H}_S$ and $\boldsymbol{H}_{\bar{S}}$ are obtained as follows by using **(4)**, **(15)**, and **(19)**

$$\boldsymbol{H}_S = \begin{bmatrix} \boldsymbol{C}_{\mathrm{AB}} & \tilde{\boldsymbol{R}}_{\mathrm{AC}}\boldsymbol{C}_{\mathrm{AB}} - \boldsymbol{C}_{\mathrm{OB}}\tilde{\boldsymbol{R}}_{\mathrm{BC}} \\ \boldsymbol{O} & \boldsymbol{C}_{\mathrm{AB}} \\ \boldsymbol{I}_3 & \boldsymbol{O} \\ \boldsymbol{O} & \boldsymbol{I}_3 \end{bmatrix} \tag{21}$$

$$\boldsymbol{H}_{\bar{S}} = \begin{bmatrix} \boldsymbol{C}_{\mathrm{AB}}\boldsymbol{V}_{\mathrm{BC}}' + \tilde{\boldsymbol{R}}_{\mathrm{AC}}\boldsymbol{\Omega}_{\mathrm{BA}}' \\ \boldsymbol{\Omega}_{\mathrm{BA}}' \\ \boldsymbol{O} \\ \boldsymbol{O} \end{bmatrix} \tag{22}$$

Finally, the equation of motion of the co-axial rotor helicopter is derived as **(3)**. Here, $\boldsymbol{m}^S$ and $\boldsymbol{f}^S$ are obtained as follows:

$$\boldsymbol{m}^S = \begin{bmatrix} \boldsymbol{M}_{\mathrm{A}} + \boldsymbol{M}_{\mathrm{B}} & \boldsymbol{C}_{\mathrm{AB}}^{\mathrm{T}}\boldsymbol{M}_{\mathrm{A}}\tilde{\boldsymbol{R}} \\ \tilde{\boldsymbol{R}}^{\mathrm{T}}\boldsymbol{M}_{\mathrm{A}}\boldsymbol{C}_{\mathrm{AB}} & \tilde{\boldsymbol{R}}^{\mathrm{T}}\boldsymbol{M}_{\mathrm{A}}\tilde{\boldsymbol{R}} + \boldsymbol{C}_{\mathrm{AB}}^{\mathrm{T}}\boldsymbol{J}_{\mathrm{A}}\boldsymbol{C}_{\mathrm{AB}} + \boldsymbol{J}_{\mathrm{B}} \end{bmatrix} \tag{23}$$

$$\boldsymbol{f}^S = \begin{bmatrix} \boldsymbol{f}_1^{ST} & \boldsymbol{f}_2^{ST} \end{bmatrix}^{\mathrm{T}} \tag{24}$$

$$\begin{aligned} \boldsymbol{f}_1^{\mathrm{S}} = -\boldsymbol{C}_{\mathrm{AB}}^{\mathrm{T}}\boldsymbol{M}_{\mathrm{A}}\{ & (\boldsymbol{C}_{\mathrm{AB}}\tilde{\boldsymbol{\Omega}}_{\mathrm{OB}}'\boldsymbol{C}_{\mathrm{AB}} + \tilde{\boldsymbol{\Omega}}_{\mathrm{BA}}'\boldsymbol{C}_{\mathrm{AB}} - \boldsymbol{C}_{\mathrm{AB}}\tilde{\boldsymbol{\Omega}}_{\mathrm{BA}}')\boldsymbol{V}_{\mathrm{OB}}' \\ & + (\boldsymbol{C}_{\mathrm{AB}}\tilde{\boldsymbol{\Omega}}_{\mathrm{OB}}'\tilde{\boldsymbol{R}} + \tilde{\boldsymbol{\Omega}}_{\mathrm{BA}}'\tilde{\boldsymbol{R}} - \tilde{\boldsymbol{R}}_{\mathrm{AC}}\boldsymbol{C}_{\mathrm{AB}}\tilde{\boldsymbol{\Omega}}_{\mathrm{BA}}' + \boldsymbol{C}_{\mathrm{AB}}\tilde{\boldsymbol{\Omega}}_{\mathrm{BA}}'\tilde{\boldsymbol{R}}_{\mathrm{BC}} - \boldsymbol{C}_{\mathrm{AB}}\tilde{\boldsymbol{V}}_{\mathrm{BC}}')\boldsymbol{\Omega}_{\mathrm{OB}}' \\ & + (\boldsymbol{C}_{\mathrm{AB}}\tilde{\boldsymbol{\Omega}}_{\mathrm{OB}}'\boldsymbol{C}_{\mathrm{AB}} + \tilde{\boldsymbol{\Omega}}_{\mathrm{BA}}'\boldsymbol{C}_{\mathrm{AB}} - \boldsymbol{C}_{\mathrm{AB}}\tilde{\boldsymbol{\Omega}}_{\mathrm{BA}}')\boldsymbol{V}_{\mathrm{BC}}' \\ & + (\boldsymbol{C}_{\mathrm{AB}}\tilde{\boldsymbol{\Omega}}_{\mathrm{OB}}'\tilde{\boldsymbol{R}}_{\mathrm{AC}} + \tilde{\boldsymbol{\Omega}}_{\mathrm{BA}}'\tilde{\boldsymbol{R}}_{\mathrm{AC}})\boldsymbol{\Omega}_{\mathrm{BA}}' \\ & + \boldsymbol{C}_{\mathrm{AB}}\dot{\boldsymbol{V}}_{\mathrm{BC}}' + \tilde{\boldsymbol{R}}_{\mathrm{AC}}\dot{\boldsymbol{\Omega}}_{\mathrm{BA}}'\} - \boldsymbol{M}_{\mathrm{B}}\tilde{\boldsymbol{\Omega}}_{\mathrm{OB}}'\boldsymbol{V}_{\mathrm{OB}}' + \boldsymbol{C}_{\mathrm{AB}}^{\mathrm{T}}\boldsymbol{F}_{\mathrm{OA}}' + \boldsymbol{F}_{\mathrm{OB}}' \end{aligned} \tag{25}$$

$$\begin{aligned} \boldsymbol{f}_2^{\mathrm{S}} = -\tilde{\boldsymbol{R}}^{\mathrm{T}}\boldsymbol{M}_{\mathrm{A}}\{ & (\boldsymbol{C}_{\mathrm{AB}}\tilde{\boldsymbol{\Omega}}_{\mathrm{OB}}'\boldsymbol{C}_{\mathrm{AB}} + \tilde{\boldsymbol{\Omega}}_{\mathrm{BA}}'\boldsymbol{C}_{\mathrm{AB}} - \boldsymbol{C}_{\mathrm{AB}}\tilde{\boldsymbol{\Omega}}_{\mathrm{BA}}')\boldsymbol{V}_{\mathrm{OB}}' \\ & + (\boldsymbol{C}_{\mathrm{AB}}\tilde{\boldsymbol{\Omega}}_{\mathrm{OB}}'\tilde{\boldsymbol{R}} + \tilde{\boldsymbol{\Omega}}_{\mathrm{BA}}'\tilde{\boldsymbol{R}} - \tilde{\boldsymbol{R}}_{\mathrm{AC}}\boldsymbol{C}_{\mathrm{AB}}\tilde{\boldsymbol{\Omega}}_{\mathrm{BA}}' + \boldsymbol{C}_{\mathrm{AB}}\tilde{\boldsymbol{\Omega}}_{\mathrm{BA}}'\tilde{\boldsymbol{R}}_{\mathrm{BC}} - \boldsymbol{C}_{\mathrm{AB}}\tilde{\boldsymbol{V}}_{\mathrm{BC}}')\boldsymbol{\Omega}_{\mathrm{OB}}' \\ & + (\boldsymbol{C}_{\mathrm{AB}}\tilde{\boldsymbol{\Omega}}_{\mathrm{OB}}'\boldsymbol{C}_{\mathrm{AB}} + \tilde{\boldsymbol{\Omega}}_{\mathrm{BA}}'\boldsymbol{C}_{\mathrm{AB}} - \boldsymbol{C}_{\mathrm{AB}}\tilde{\boldsymbol{\Omega}}_{\mathrm{BA}}')\boldsymbol{V}_{\mathrm{BC}}' \\ & + (\boldsymbol{C}_{\mathrm{AB}}\tilde{\boldsymbol{\Omega}}_{\mathrm{OB}}'\boldsymbol{J}_{A} + \tilde{\boldsymbol{\Omega}}_{\mathrm{BA}}'\boldsymbol{J}_{A})\boldsymbol{\Omega}_{\mathrm{BA}}' \\ & + \boldsymbol{J}_{A}\dot{\boldsymbol{\Omega}}_{\mathrm{BA}}'\} - \tilde{\boldsymbol{\Omega}}_{\mathrm{OB}}'\boldsymbol{J}_{\mathrm{B}}\boldsymbol{\Omega}_{\mathrm{OB}}' + \tilde{\boldsymbol{R}}^{\mathrm{T}}\boldsymbol{F}_{\mathrm{OA}}' + \boldsymbol{C}_{\mathrm{AB}}^{\mathrm{T}}\boldsymbol{N}_{\mathrm{OA}}' + \boldsymbol{N}_{\mathrm{OB}}' \end{aligned} \tag{26}$$

Additionally, $\tilde{\boldsymbol{R}}$ is defined as

$$\tilde{\boldsymbol{R}} = \tilde{\boldsymbol{R}}_{\mathrm{AC}}\boldsymbol{C}_{\mathrm{AB}} - \boldsymbol{C}_{\mathrm{AB}}\tilde{\boldsymbol{R}}_{\mathrm{BC}} \tag{27}$$

Table 2 – Specifications of Unmanned Helicopter

Mass of mission unit	66 [kg]
Inertia moment of mission unit	diag(50, 50, 50) [kg m^2]
Mass of frame unit	100 [kg]
Inertia moment of frame unit	diag(50, 50, 50) [kg m^2]
Distance between COG of mission unit and joint	0.206 [m]
Distance between COG of frame unit and joint	0.693 [m]

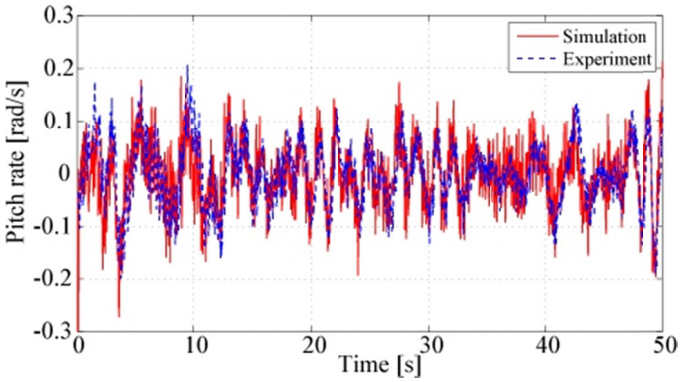


Figure 6 – Comparison of pitch angular velocity

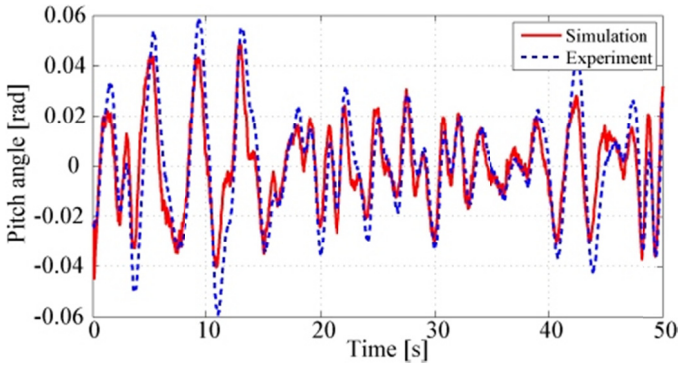


Figure 7 – Comparison of pitch angle

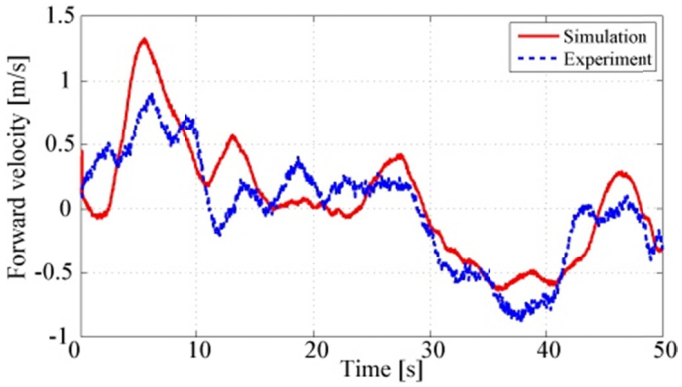


Figure 8 – Comparison of forward velocity

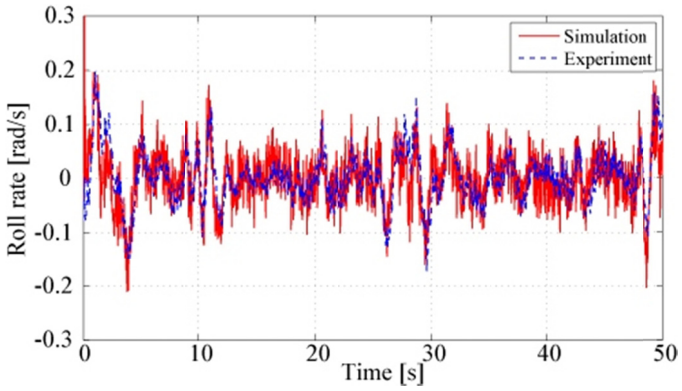


Figure 9 – Comparison of roll angular velocity

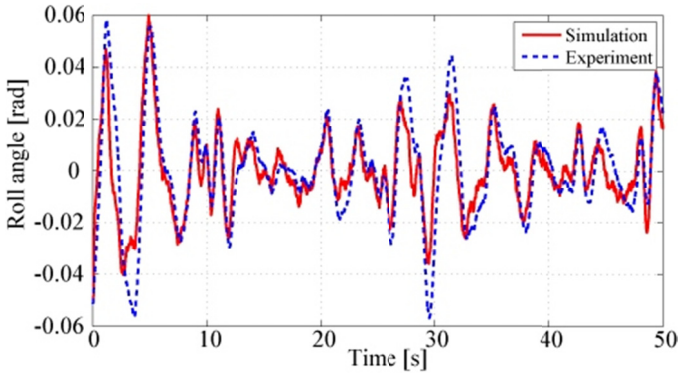


Figure 10 – Comparison of roll angle

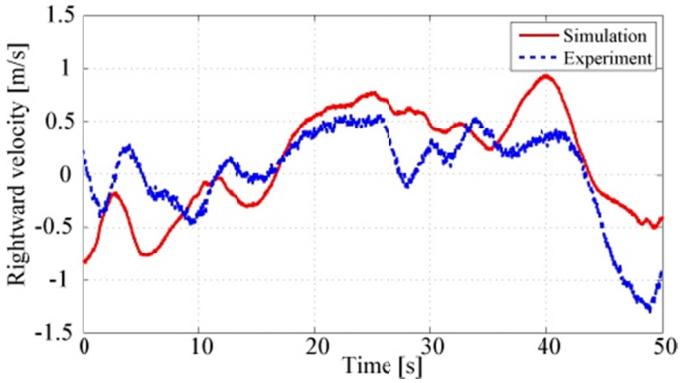


Figure 11 – Comparison of rightward velocity

To verify the validity of derived model, a simulation was conducted by using the equation of motion. In the simulation, the outputs of the model are compared with the experimental data. Model parameters used in this simulation are listed in **Table 2**. All the forces and moments in **(8)-(10)**, which are impressed into the helicopter, were derived in consideration of the aerodynamics of co-axial rotors. *Blade Element Theory* and *Momentum Theory* in **[11]-[12]** were used to obtain thrust and torque of the rotors. The gravity was also included in **(8)-(10)**. Moreover, $\boldsymbol{V}'_{BC}$, $\boldsymbol{\Omega}'_{BA}$ and the time derivatives of them were determined by the motion of the tilting and shifting mechanisms. They are considered as the inputs of the model.

Figure 6 - Figure 11 show the results of the simulation for horizontal motion. In these figures, the solid line represents the output of the mathematical model; dashed line represents flight experiment data measured by sensors, which are mounted on the helicopter. **Figure 6** and **Figure 9** show the pitching and rolling angular velocity of the helicopter measured by using gyro sensor. **Figure 7** and **Figure 10** show the pitching and rolling attitude angle measured by the attitude sensor. **Figure 8** and **Figure 11** show the horizontal velocity measured by GPS. From **Figure 6**, **Figure 7**, **Figure 9**, and **Figure 10**, the model outputs accords with the experimental data in the case of angular velocity and attitude angle. Accordingly, it seems that attitude dynamics of the helicopter could be expressed precisely by the mathematical model. However, in the case of horizontal velocity, the model outputs do not accord with experimental data well. The reason of mismatch seems to be the influence of aerodynamics which was not considered in the

simulation. In fact, we have not yet considered the imbalance of lift force on the disc which causes pitch-up phenomenon. Moreover, we also have not yet considered vertical and yawing motion. Therefore, we should implement them into the simulation in future works.

IV. Motion Analysis

To know the relation between the motion and mechanical specification of the helicopter, we conducted motion analysis by using derived mathematical model. Although the dynamics of horizontal velocity have not yet been expressed well by the model, we conclude that the attitude model is precise enough to use motion analysis. Therefore, only attitude motion of the helicopter is analyzed in this section. For operation of the helicopter, reducing the vibration of the frame unit is the most important because some payloads such as a camera, sensors for application, and a product is mounted on the frame unit. For this reason, we examine the optimal position of the universal joint to reduce vibration of the frame unit by simulation. In the simulation, we impressed the input to the tilting mechanism as sinusoidal signal, and the input to shifting mechanism is zero. Simultaneously, we record the amplitude of the attitude of the frame unit in steady state. This simulation was carried out repeatedly while changing the frequency of the input to the tilting mechanisms and the position of the universal joint. Meanwhile, the distance between COG of the frame unit and the COG of the mission unit ($l + d$ in **Figure 5**) was fixed at 1 m in the simulation.

Figure 12 shows the examination result of the optimal position of the universal joint. In this figure, the lateral axis represents the frequency of the input to the tilting mechanism, the longitudinal axis represents the amplitude of the attitude of the frame unit in steady state. Moreover, notation *d* represents the distance between COG of the frame unit and the universal joint as shown in **Figure 5**. From the figure, it is shown that the amplitude of the attitude of the frame unit is largest when the input frequency is between 0.1-0.2 Hz. It means that the helicopter has the resonance frequency at 0.1-0.2 Hz. Moreover, it is clear from the figure that the amplitude of the frame unit is affected drastically by the position of the universal joint, and the maximum of the amplitude could be suppressed by changing the position of the universal joint. To find the optimal position of the universal joint, examination was carried out in detail between 0.1-0.2 Hz. The result is shown in **Figure 13**.

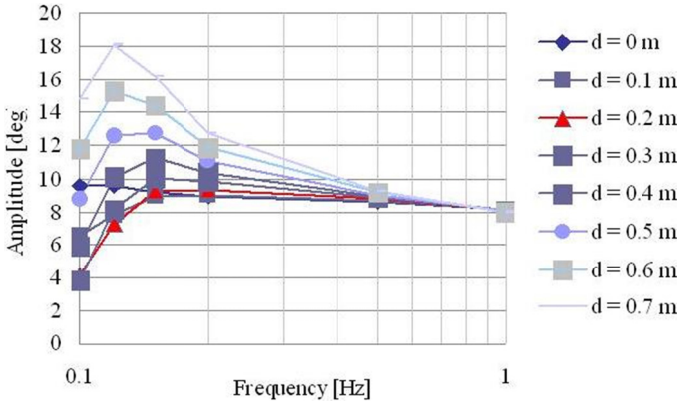


Figure 12 – Examination of the position universal joint

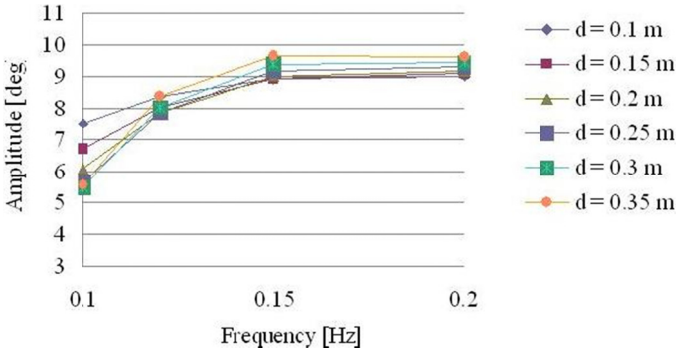


Figure 13 – Examination of the position universal joint (close-up)

From the figure, the maximum of the amplitude of the frame unit could be smallest when the distance between COG of the frame unit and the universal joint is 0.2 m. As a result, we conclude that the optimal position of the universal joint for reducing vibration of the frame unit is 0.2 m from COG of the frame unit.

V. Concluding Remarks

In this paper, we derived the mathematical model of fixed-pitch co-axial rotor unmanned helicopter by using multi-body dynamics modeling technique. We applied the velocity transformation method to derive the equation of motion of the helicopter. Verification of the model is conducted by comparing the flight experiment data with model output. Finally, fundamental motion analysis for reducing vibration of the frame unit was performed by using derived mathematical model.

In future woks, we implement the aerodynamic effect of the co-axial rotor which cannot be considered in current model such as the interference of each rotor, vertical motion, and yaw motion to the mathematical model to realize more precise simulation and motion analysis.

Acknowledgment

This work was partly supported by JSPS KAKENHI Grant Number 24760185.

References

[1] B. Mettler, M. B. Tischler, and T. Kanade, "System Identification Modeling of A Small Scale Unmanned Rotorcraft for Flight Control Design," *Journal of American Helicopter Society*, vol. 47, no. 1, 2002, pp. 50–63.

[2] J. H. Lee, B. M. Min, and E. T. Kim, "Autopilot Design of Tilt-Rotor UAV using Particle Swarm Optimization Method," *Proceedings of 2007 International Conference on Control, Automation and Systems*, 2007, pp. 1629–1633.

[3] C. Bermes, S. Leutenegger, S. Bouabdallah, D. Schafroth, and R. Siegwart, "New Design of The Steering Mechanism for a Mini Coaxial Helicopter," *Proceedings of IEEE International Conference on Intelligent Robots and Systems*, 2008, pp. 1236-1241.

[4] S. Shen, N. Michael, and V. Kumar, "Autonomous Milti-Floor Indoor Navigation with A Computationally Constrained MAV," Proceedings of IEEE International Conference on Robotics and Automation, 2011, pp. 20-25

[5] http://www.kamov.ru/en/

[6] T. Ishii, S. Suzuki, G. Yanagisawa, K. Tomita, Y. Yokoyama, "Multi-Body Dynamics Modeling of Fixed-pitch Co-axial Rotor Unmanned Helicopter," *Proceedings of International Conference on Intellignent Unmanned Systems 2011*, 2011

[7] H. Tajima, *Fundamental of Multibody Dynamics*, Tokyo Denki University Press, 2006, (in Japanese)

[8] A. A. Shabana, *Dynamics of Multibody Systems 3rd Edition*, Cambridge, 2005

[9] W. Jekkovsky, "The Structure of Multibody Dydnamics Equations," *Journal of Guidance and Control*, vol. 1, no. 3, 1978, pp. 173-182

[10] S. S. Kim, and M. J. Vanderploeg, "A General and Efficent Method for Dynamics Analysis of Mechanical System Using Velocity Transformation," *ASME Journal of Mechanisms, Transmissions, and Automation Design*, vol. 108, 1986, pp. 176-182

[11] A. R. S. Bramwell, G. Done, and D. Balmford, *Bramwell's Helicopter Dynamics*, AIAA, 2001

[12] H. Glauert, *A General Theory of the Autogyro*, Aeronautical Research Council R&M 1111, 1926